International Journal of Pharmaceutics, 15 (1983) 335–345
Elsevier

Pharmacokinetics and distribution of a biodegradable drug-carrier

L. Grislain *, P. Couvreur *, V. Lenaerts *, M. Roland *, D. Deprez-Decampeneere ** and P. Speiser ***

* *Laboratoire de Pharmacie Galénique, and ** International Institute of Cellular and Molecular Pathology, Université Catholique de Louvain, B-1200 Bruxelles (Belgium) and *** School of Pharmacy, Federal Institute of Technology, Zürich (Switzerland)*

(Received December 20th, 1982)
(Accepted January 14th, 1983)

Summary

This paper describes tissue distribution, blood clearance and excretion of biodegradable cyanoacrylic nanoparticles.

After intravenous administration, nanoparticles were rapidly cleared from the blood stream and concentrated mainly in the reticuloendothelial system. When administrated subcutaneously, nanoparticles seemed to avoid the liver and the spleen whereas they concentrated in the gut wall.

Whole body autoradiography performed on Lewis Lung carcinoma-bearing mice showed progressive accumulation of the carrier in tumoral tissue. Furthermore a high level of radioactivity was found in the metastatic lungs of cancerous animals, whereas no lung accumulation was observed in healthy mice. Data are given concerning the enzymatic contribution to the degradation of the nanoparticles in vivo

Introduction

Recently, we developed a drug colloidal carrier made of polyalkylcyanoacrylate having a diameter of about 0.2 μm (Couvreur et al., 1978; Couvreur et al., 1979a and b). Due to their polymeric nature, these small particles may be more stable than liposomes in biological fluids and have a longer shelf-life (Kimelberg et al., 1975; Couvreur et al., 1979b). Another advantage is that these particles are more or less quickly degraded depending on the length of their alkyl chain (Couvreur et al., 1979b; Leonard et al., 1966; Vezin et al., 1980). This carrier is able to adsorb with

0378-5173/83/$03.0

high efficiency a large variety of drugs in a stable and reproducible way (Couvreur et al., 1980a). Also, it has been demonstrated that these particles can profoundly modify the distribution pattern of some anticancer drugs (Couvreur et al., 1980b; Kante et al., 1980).

Recently, we described preliminary results indicating that the use of polymethylcyanoacrylate nanoparticles as drug-carrier considerably increased the anticancer activity of dactinomycin towards experimental subcutaneous sarcoma of the rat (Brasseur et al., 1978). It is furthermore postulated that these particles could be of interest in the field of long-acting insulin therapy (Couvreur et al., 1980c). The first toxicological data obtained at the cellular and in vivo levels did not demonstrate any acute toxicity able to hinder the use of polyalkylcyanoacrylate nanoparticles in human medicine (Kante et al., 1982). Indeed, the possibility of reducing significantly the toxicity of doxorubicin by fixing it on polyisobutylcyanoacrylate nanoparticles has been demonstrated (Couvreur et al., 1982a).

It was important, however, to determine pharmacokinetic parameters, whole-body distribution and tumor localization after intravenous administration of the carrier alone. Likewise, this paper describes the influence of nanoparticles routes of administration on these pharmacological parameters. Finally, we demonstrate the enzymatic contribution to the degradation of nanoparticles.

Materials and Methods

Materials

Radioactive monomer was purchased from I.R.E. (Institut des Radioéléments, Fleurus, Belgium). Cold monomer was kindly obtained from Loctite (Dublin, Ireland).

The chemicals used for radiation counting (Instagel and Carbomax) were respectively obtained from Packard Instruments S.A. Benelux (Brussels, Belgium) and from Lumac (Basel, Switzerland).

Other chemical compounds were of reagent grade and used as purchased. The radiosensitive films (Curix) were obtained from Agfa Gevaert (Brussels, Belgium).

Preparation of radioactive monomer

Radioactive isobutyl-2-cyanoacrylate monomer was prepared according to a previously published method (McKeever, 1959). [^{14}C]Formaldehyde was used in the synthesis, which resulted in the monomer being tagged on the number three carbon atom. The radioactive monomer specific activity was 1.4 mCi/ml of monomer.

Preparation of radioactive nanoparticles

To a 10 ml aqueous solution of 4.8×10^{-3} M citric acid and 1.4×10^{-4} M dextran 70, 120 μl of radioactive monomer were added under mechanical stirring. After polymerization (at least 2 h), the nanoparticles were obtained as a milky suspension displaying a Tyndall effect. To avoid the simultaneous presence of soluble monomer, the nanoparticle suspension was centrifuged for 2 h at 20,000 rpm.

The supernatant was discarded while the nanoparticles were resuspended in distilled water under ultrasonic stirring during 1 min. The colloidal suspension was neutralized with 0.1 M NaOH and brought to isotonicity with NaCl before each animal administration.

Nanoparticle size estimations were performed using a nano-sizer counter based on the scattering of light arising from a laser source.

In vitro degradation test

One ml of a radioactive nanoparticle suspension was incubated at 37°C in 100 ml portions of 10^{-3} M EDTA–0.25 M sucrose solution adjusted to pH 5.2 by 0.1 M NaOH. This pH was chosen because cellular uptake of nanoparticles involves the lysosomal compartment. The 3 h incubation period took place in a closed container, with or without 2% liver extract concentration. The liver homogenization was performed in the sucrose–EDTA buffer solution with a Potter homogenizer rotating at 1400 rpm for 30 s at 4°C.

Nanoparticle incubation samples (5 ml) were taken out at various times, acidified with 1 N HCl and cooled to 4°C in order to stop chemical and biological degradation of the polymer. After centrifugation at 20.000 rpm for 2 h the radioactivity corresponding to intact and degraded polymer was measured by scintillation counting (Philips model PW 4510, Brussels, Belgium) in the sediment and the supernatant, respectively.

Animals

Female NMRI and C57 black mice were used.

Blood clearance and excretion of [^{14}C]nanoparticles

0.3 ml radioactive nanoparticle suspension was intravenously injected in the tail vein of mice weighing between 20 and 22 g. The animals were killed at various times; blood samples (100 µl) were collected, treated by a tissue sample oxydizer (Oxymat, IN-Intertechnique, Plaisir, France) and radioactivity was measured by scintillation counting.

4 groups of 5 mice each were injected with the same dose as described above. Each group was put in a metabolic cage and radioactivity was determined from 1 to 7 days in urine and faeces collections.

Whole body autoradiography methods

Whole body autoradiography was performed according to the method described by Ullberg (Ullberg et al., 1954). After injection of 2.5 µCi of radioactive nanoparticles, mice were killed at various times, frozen by immersion in liquid nitrogen and embedded in a 2% solution of carboxymethylcellulose. They were then sectioned with a cryomat (Cryotome 1714, Leitz, Wetzlar, F.R.G.); sagittal sections 40 µm thick were taken on adhesive tape and dried in a cold-room. All sections were pressed in the same conditions against a radiosensitive film for 4 weeks.

Quantitative tissue distribution methods

Different organs (liver, heart, spleen, lung and kidney) were removed from mice

at various times (5 min, 30 min, 4 h, 24 h) after intravenous administration of 0.3 ml of radioactive nanoparticles. After weighing, the tissue samples were treated by the oxidizer and radioactivity was measured by scintillation counting.

Tumor transplantation procedure

Female C_{57} black mice (Charles River, Cléon, France) were inoculated subcutaneously with Lewis Lung carcinoma cells, obtained from a subcutaneous primary tumor and maintained in culture. The animals received 5×10^5 cells on day 0 and were used for the quantitative tissue distribution experiment on day 14.

Results and Discussion

Blood clearance

After intravenous administration of [^{14}C]nanoparticles (0.254 μm), a rapid clearance was noted which followed a monoexponential curve (Fig. 1). After computing the results following a non-linear regression technique ("steepest descent") monocompartimental parameters were determined. Half-life ($T_{1/2}$), as calculated from the slope of the curve, was equal to 6.63 min. Volume of distribution (V_D) and total clearance (C_t) corresponded to values of 2.47 ml and 0.26 ml/min, respectively.

Urinary and faecal excretion data

Radioactivity excreted in the urine and faeces was measured 1, 3 and 7 days after

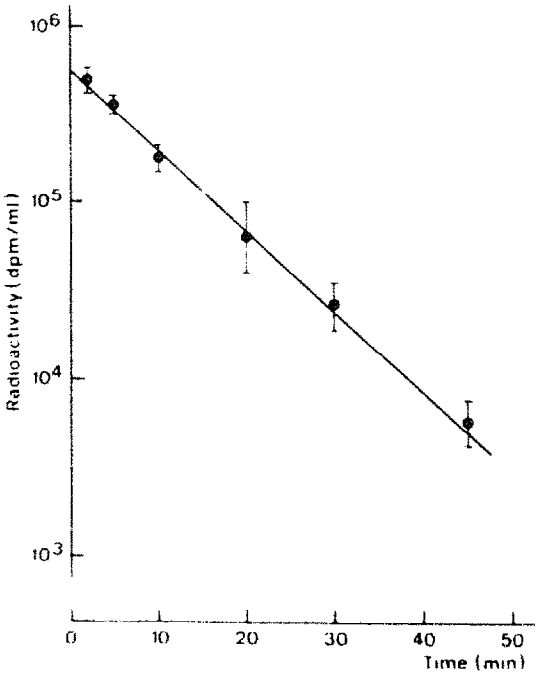

Fig. 1. Disappearance of radioactivity from blood after injection of radioactive nanoparticles into mice.

TABLE 1

URINARY AND FAECAL EXCRETION (% of injected dose) OF 0.254 μm [^{14}C]-LABELED NANOPARTICLES

Time (days)	Urinary excretion (%) ± S.D.	Faecal excretion (%) ± S.D.
1	39.9 ± 12.5	16.2 ± 4.1
3	56.4 ± 7.9	22.9 ± 6.0
7	66.6 ± 5.7	27.0 ± 6.0

The table shows arithmetic means ± S.D. obtained from 4 groups of 5 mice each.

intravenous administration of 0.254 μm nanoparticles (Table 1). The major part of radioactivity was eliminated within 7 days after injection.

Whole body autoradiography

Five minutes after intravenous administration of [^{14}C]-labeled nanoparticles radioactivity was mainly localized in the liver, the lungs and the kidneys (Fig. 2a). At this time, radioactivity was still present in the intravascular compartment (heart and blood vessels). After 30 min, blood and lung radioactivity had greatly decreased

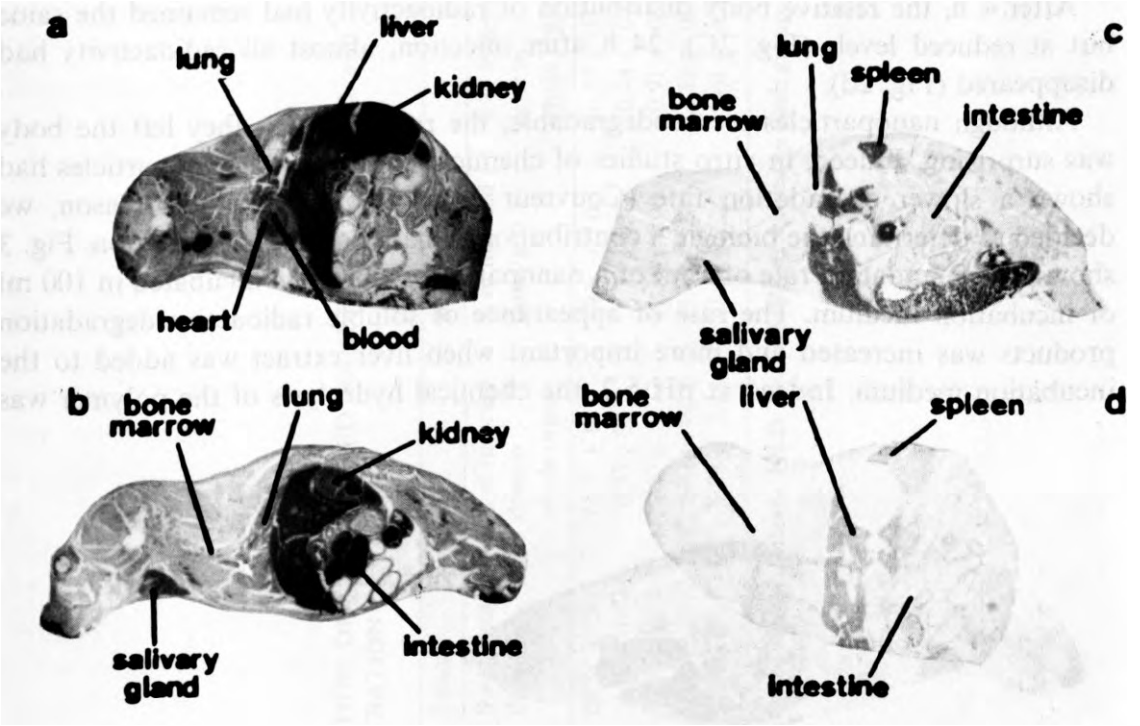

Fig. 2. Whole body autoradiography of a mouse after intravenous administration of [^{14}C]-labelled nanoparticles (mean diameter: 0.254 μm). a = 5 min; B = 30 min; C = 4 h; D = 1 day.

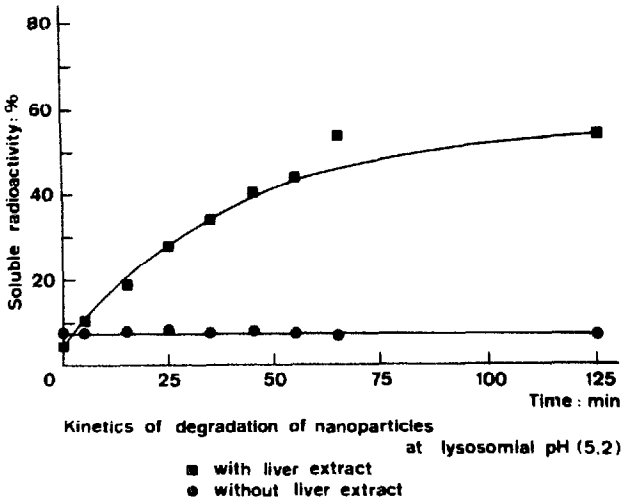

Fig. 3. Nanoparticle degradation kinetics at pH = 5.2 with (■) and without (●) liver extract.

(Fig. 2b). The kidney presented a radioactive level as strong as the liver. This phenomenon could be due to the urinary excretion of radioactive nanoparticles metabolites. At the same time, the spleen, the salivary glands and the bone marrow appeared more slightly marked, while, an important intestinal excretion had taken place.

After 4 h, the relative body distribution of radioactivity had remained the same but at reduced levels (Fig. 2C). 24 h after injection, almost all radioactivity had disappeared (Fig. 2d).

Although nanoparticles are biodegradable, the rate at which they left the body was surprising. Indeed, in vitro studies of chemical hydrolysis of nanoparticles had shown a slower degradation rate (Couvreur et al., 1979b). For this reason, we decided to determine the biological contribution to nanoparticles degradation. Fig. 3 shows the degradation rate of 1 ml of a nanoparticle suspension incubated in 100 ml of incubation medium. The rate of appearance of soluble radioactive degradation products was increased and more important when liver extract was added to the incubation medium. Indeed at pH 5.2, the chemical hydrolysis of the polymer was

Fig. 4. Whole body autoradiography of a mouse after subcutaneous injection of [^{14}C]-labelled nanoparticles (mean diameter: 0.254 μm) 30 min after administration.

TABLE 2

DISTRIBUTION OF [^{14}C]-LABELED NANOPARTICLES (0.257 μm) IN THE LIVER, HEART, SPLEEN, KIDNEY AND LUNG AFTER i.v. ADMINISTRATION

Organ	5 min		30 min		4h		24 h	
	% of injected dose/g	% of injected dose in whole organ	% of injected dose/g	% of injected dose in whole organ	% of injected dose/g	% of injected dose in whole organ	% of injected dose/g	% of injected dose in whole organ
Liver	61.5 ±15	78.7 ±11	49.6 ±7.0	66.37±15	25.04±4.9	42.1 ±6.3	7.9 ±3.0	11.9 ±4.8
Heart	6.5 ±0.87	0.73±02	4.3 ±0.95	0.44± 0.05	3.25±0.58	0.30±0.04	1.5 ±0.6	0.15±0.04
Spleen	15.7 ± 2.6	1.53± 0.12	11.38±4.00	0.91± 0.21	11.7 ±2.5	0.91±0.21	6.13±2.7	0.57±0.12
Kidney	17.99± 4.7	5.73± 0.12	11.49±3.7	3.58± 0.73	3.6 ±0.60	0.61±0.13	1.44±0.31	0.23±0.05
Lung	15.0 ± 2.5	5.38± 2.18	17.47±2.2	3.01± 0.49	12.48±1.5	2.4 ±0.23	5.26±3.79	1.18±0.81

The table shows arithmetic means ± S.D. obtained from 4 mice in each group.

weak, whereas an important enzymatic degradation remained (Fig. 3).

After subcutaneous injection, the overall rate of whole body distribution of the radioactivity was lower than after intravenous administration. After 30 min, the site of injection remained deeply marked, and resorbed radioactivity concentrated in the gut wall (Fig. 4). It is important to note the lack of detectable radioactivity in the liver. When nanoparticles were injected intramuscularly, the same distribution pattern was repeated.

Quantitative tissue distribution (Table 2)

Autoradiography data were quantitatively confirmed by tissue counting. After intravenous administration of [^{14}C]nanoparticles, the radioactivity was mainly localized in the liver. Indeed, after 5 min, 78% of injected radioactivity was found in the liver. The total amount of radioactivity measured in other analyzed tissues reached a maximum level of 13% at the same time after injection.

Radioactivity decreased progressively in all tested organs during 24 h.

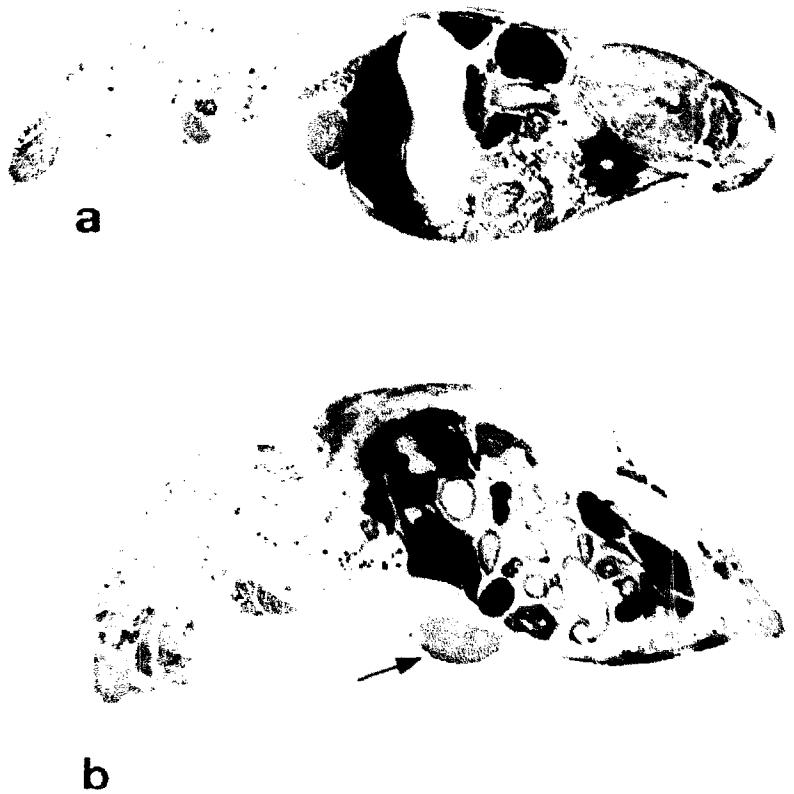

Fig. 5. Whole body autoradiography of subcutaneous Lewis Lung carcinoma (→) bearing-mouse (b) and healthy mouse (a) 4 h after intravenous administration of [^{14}C]nanoparticles.

TABLE 3

LUNG AND LIVER CONCENTRATION OF RADIOACTIVITY 4 h AFTER INTRAVENOUS ADMINISTRATION OF [^{14}C]NANOPARTICLES (2.5 μCi) TO HEALTHY (A) AND TUMOR-BEARING MICE (B)

	Lung	Liver	Lung/liver
A	10.7 ± 1.9	26.4 ± 5.0	0.41 ± 0.13
B	67.9 ± 10.5	12.9 ± 1.0	5.26 ± 1.11

The values represented the mean and the standard deviation of 7 animals in each group.

Tumor localization

Whole body autoradiography was performed on C57 black mice with subcutaneously implanted Lewis Lung carcinoma. The goal was to determine the intratumoral localization and concentration of the carrier.

From 5 min until 4 h after intravenous administration of [^{14}C]nanoparticles, progressive accumulation occurred in the tumoral tissue and reached, after 4 h, a level as strong as for the salivary glands (Fig. 5a). Furthermore, the tumor nodule was obviously more marked than the normal underlying tissue.

Intratumour accumulation of nanoparticles occurred after disappearance of the carried from the blood stream. This observation confirms the localization of the carrier inside the sarcoma and implies a possible passage of the submicroscopic particles through the vascular endothelium. Furthermore, we observed a higher level of radioactivity in the lung tissue of tumor-bearing mice (Fig. 5a). It is important to note the lack of radioactivity in the healthy animal 4 h after injection (Fig. 5b). These observations were quantitatively confirmed by measuring the radioactivity in lung and liver. Indeed, in the case of tumor-bearing mice, the lung radioactivity was 6 times higher than for the lungs of healthy animals (Table 3). Furthermore this radioactivity enhancement seemed to occur to the detriment of the liver (Table 3).

Conclusions

The extravascular distribution of polyalkylcyanoacrylate nanoparticles is rapid after intravenous administration. The carrier concentrates in organs rich in reticuloendothelial cells (liver, spleen and bone marrow). The high radioactive concentration in the kidneys and in the gut implies that excretion occurs through the urine and faeces. The rapid disappearance of the nanoparticles from the body, as observed on the autoradiograms and quantitatively confirmed by tissue scintillation counting was surprising with regard to the speed of chemical hydrolysis of the carrier as previously published (Couvreur et al., 1979b). The present results demonstrate an important enzymatic contribution to the degradation of the nanoparticles and can explain that most of the carrier is cleared from the body after 24 h. In contrast to intravenous administration, subcutaneous injections seem to by-pass the liver. The rate of radioactivity decrease from the site of injection is slow and then seems to concentrate exclusively in the gut-wall.

The great problem of colloidal drug carriers consists in the passage through the endothelial barrier to sites other than the liver and spleen. We demonstrated the possibility of such passage of polyisobutylcyanoacrylate nanoparticles in a neoplastic tissue. Indeed, tumor concentration of the carrier is maximum when nanoparticles have totally disappeared from the blood stream. This tissular capture of the carrier through blood vessel endothelium could be explained by a change in the structure of the capillary wall due to inflammatory process at the tumor site.

However, the most interesting observation remains in the intense pulmonary capture of the carrier in tumor-bearing animals. Because subcutaneously grafted Lewis Lung carcinoma easily induces metastasis in the lung, and because of the lack of such carrier concentration in pulmonary tissue of healthy animals, this phenomenon could be a valuable reason to justify the use of nanoparticles as a drug carrier for pulmonary metastasis treatment. Further confirmation of this peculiar advantage will be undertaken by testing the anticancer activity of various cytostatic drugs linked to polyalkylcyanoacrylate nanoparticles on experimental Lewis Lung carcinoma.

These experiments suggest that nanoparticles may be a valuable drug-carrier candidate able to concentrate in specific target sites. Furthermore, their rapid body elimination as well as their degradability avoid side-effects due to long-lasting accumulation in several tissues.

Acknowledgements

This work was supported by the SOPAR S.A. Company, by the Institut pour l'Encouragement de la Recherche Scientifique dans l'Industrie et l'Agriculture (I.R.S.I.A.) and by the Fonds National de la Recherche Scientifique Belge (F.N.R.S.). The kind support of the Assurances Générales de France was greatly appreciated. The authors wish to thank Mrs. Duhamel for her excellent technical assistance and Mr. Vandiest for the drawings and the photographic work. The authors are also thankful to Dr. Cumps for competent computing of the pharmacokinetic data. The valuable advice of Mr. Pellegrin (Laboratoire de Pharmacologie, Université Catholique de Louvain) concerning the tissue samples preparation proved to be essential.

References

Brasseur, F., Couvreur, P., Kante, B., Deckers-Passau, L., Roland, M., Deckers, C. and Speiser, P., Actinomycin D adsorbed on polymethylcyanoacrylate nanoparticles. Eur. J. Cancer, 16 (1978) 1441–1445.

Couvreur, P., Kante, B. and Roland, M., Les perspectives d'utilisation des formes microdispersées comme vecteurs intracellulaires. Pharm. Acta Helv., 53 (1978) 341–347.

Couvreur, P., Kante, B., Roland, M., Guiot, P., Baudhuin, P. and Speiser, P., Polycyanoacrylate nanocapsules as potential lysosomotropic carriers: preparation, morphological and sorptive properties. J. Pharm. Pharmacol., 31 (1979a) 331–332.

Couvreur, P., Kante, B., Roland, M. and Speiser, P., Adsorption of antineoplastic drugs to polyal-

kylcyanoacrylate nanoparticles and their release characteristics in a calf serum medium. J. Pharm. Sci., 68 (1979b) 1521–1524.

Couvreur, P., Kante, B. and Roland, M., Les vecteurs lysosomotropes. J. Pharm. Belg., 35 (1980a) 51–60.

Couvreur, P., Kante, B., Lenaerts, V., Scailteur, V., Roland, M. and Speiser, P., Tissue distribution of antitumors drugs associated to polyalkylcyanoacrylate nanoparticles. J. Pharm. Sci., 69 (1980b) 199–201.

Couvreur, P., Lenaerts, V., Kante, B., Roland M. and Speiser, P., Oral and parenteral administration of insulin associated to hydrolysable nanoparticles. Acta Pharm. Technol., 26 (1980c) 220–222.

Couvreur, P., Kante, B., Grislain, L., Roland, M. and Speiser, P., Toxicity of polyalkylcyanoacrylates nanoparticles II. Doxorubicin loaded nanoparticles. J. Pharm. Sci., 7 (1982a) 790–792.

Couvreur, P., Roland, M. and Speiser, P., United States Patent, no. 4329332, 1982b.

Kante, B., Couvreur, P., Lenaerts, V., Guiot, P.,Roland, M. and Speiser, P., Tissue distribution of [^{3}H]actinomycin-D adsorbed on polybutylcyanoacrylate nanoparticles. Int. J. Pharm., 7 (1980) 45–53.

Kante, B., Couvreur, P., Dubois-Crack, G., De Meester, C., Roland, M., Mercier, M. and Speiser, P., Toxicity of polyalkylcyanoacrylate nanoparticles I. Free nanoparticles. J. Pharm. Sci., 71 (1982) 786–790.

Kimelberg, H.K., Mayhew, E. and Papahajopoulos, P., Distribution of liposome-entrapped cations in tumor bearing mice. Life Sci., 17 (1975) 715–724.

Leonard, F., Kulkarni, R.K., Brandes, G., Nelson, J. and Cameron, J., Synthesis and degradation of poly(alkyl α-cyanoacrylates). J. Appl. Polym. Sci., 19 (1966) 259–272.

McKeever, C.M., Preparation of alkyl-α-cyanoacrylates, U.S. Patent 2, 919, 1959.

Ulberg, S., Studies on the distribution and fate of S^{35}-labelled benzylpenicillin in the body. Acta Radiol., 118 (1954) 1–31.

Vezin, W.R., and Florence, T.A., In vitro heterogeneous degradation of poly(*n*-alkyl α-cyanoacrylates). J. Biomed. Mat. Res., 14 (1980) 93–106.